Using memory-efficient algorithm for large-scale time-domain modeling of surface plasmon polaritons propagation in organic light emitting diodes

Andrey Zakirov[1,2], Sergei Belousov[2,4], Ilya Valuev[2,3,6], Vadim Levchenko[1], Anastasia Perepelkina[1,5], Yasunari Zempo[5]

[1] Keldysh Institute of Applied Mathematics, Moscow, 125047, Russia;
[2] Kintech Lab Ltd., Moscow, 123298, Russia; [3] HiperCone Ltd., Moscow, 123298, Russia;
[4] National Research Center "Kurchatov Institute" 123182, Moscow, Russia; [5] Hosei University, Faculty of Computer and Information Sciences, Tokyo, 184-8584, Japan
[6] Joint Institute for High Temperatures, Moscow, 125412, Russia

E-mail: mogmi@narod.ru

Abstract. We demonstrate an efficient approach to numerical modeling of optical properties of large-scale structures with typical dimensions much greater than the wavelength of light. For this purpose, we use the finite-difference time-domain (FDTD) method enhanced with a memory efficient Locally Recursive non-Locally Asynchronous (LRnLA) algorithm called DiamondTorre and implemented for General Purpose Graphical Processing Units (GPGPU) architecture. We apply our approach to simulation of optical properties of organic light emitting diodes (OLEDs), which is an essential step in the process of designing OLEDs with improved efficiency. Specifically, we consider a problem of excitation and propagation of surface plasmon polaritons (SPPs) in a typical OLED, which is a challenging task given that SPP decay length can be about two orders of magnitude greater than the wavelength of excitation. We show that with our approach it is possible to extend the simulated volume size sufficiently so that SPP decay dynamics is accounted for. We further consider an OLED with periodically corrugated metallic cathode and show how the SPP decay length can be greatly reduced due to scattering off the corrugation. Ultimately, we compare the performance of our algorithm to the conventional FDTD and demonstrate that our approach can efficiently be used for large-scale FDTD simulations with the use of only a single GPGPU-powered workstation, which is not practically feasible with the conventional FDTD.

1. Introduction

Improvement of optical devices design by numerical simulation is generally less expensive than multiple iterative trial fabrication. However, the simulation methods are often limited by the computational power. Particularly, full-wave optical simulation requires fine space and time meshes. The treatment of the whole device in such conditions implies large memory and computing performance, which is on the threshold of the current computer technology, or even far beyond it. So there exists a range of problems that has not been solved numerically yet due to computer cost limitations, such as a whole-device full wave simulation of OLED [1], optical antennae, and others [2].

In this work we demonstrate the practical usage of a high performance FDTD [2] code

DTmaxwell [3]. The aim of its development was to fully utilize the computational performance of a GPGPU-powered computer (single node or cluster) so that by minimizing the computation time and reformulating memory requirements we may broaden the scope of simulated problems in the area of electromagnetic modeling. DTmaxwell was developed on the base of finite-difference time domain algorithm DiamondTorre [4, 5] for CUDA GPGPU. DiamondTorre belongs to the class of Locally-Recursive non-Locally Asynchronous (LRnLA) algorithms and will be explained briefly in the following sections. DTmaxwell code implements all necessary typical features for FDTD simulation:

- use of GPGPU accelerators;
- 3D geometry;
- 4th order approximation for finite differences in space; 2nd order approximation in time;
- Perfectly Matched Layer (PML) boundaries [6];
- Total Field/Scattered Field (TF/SF) source;
- arbitrary model for material equations, including Drude-Lorenz model for metals;
- performance of 1 billion Yee cells updates per second on one GPU;
- linear scalability on multi-GPU clusters.

Previously, we have studied the code performance and scalability [7]. High computation rate of more than 1 billion Yee cell updates per second on one device was achieved. The scaling for ~ 1000 devices is linear for weak scaling, and saturates at ~ 100 for strong scaling. The maximal achieved performance on a TSUBAME 2.5 supercomputer was $0.65 \cdot 10^{12}$ Yee Cells per second for a 3D domain with $0.3 \cdot 10^{12}$ Yee cells in total. This number of cells corresponds, for example, to 1 cubic millimeter domain for wave optics problems.

In this work, we apply DTmaxwell code for modeling of optical properties of OLEDs. We take our previous work as the base for the current study: [8] describes a numerical investigation of an OLED by the FDTD code EMTL [9]. Presently we use the problem described in the mentioned paper as a test case for assessing capabilities and performance of DTmaxwell code, and for comparing the results and performance with EMTL, which utilizes traditional FDTD time stepping algorithm.

2. Problem statement

OLEDs are multilayered electroluminescent devices [10]. Light emission is generated via the recombination of excitons in the organic layer in the close proximity to the metallic cathode. The generated emission excites SPPs at the surface of the metallic cathode in OLEDs thus creating a major loss channel leading to the low outcoupling efficiency seen in these devices [8]. One of the methods used to increase the light outcoupling efficiency of OLEDs consists in extracting the energy lost to SPPs via corrugation at the cathode surface. SPPs scatter off the corrugation as they propagate along the metal-organic interface thereby recovering the light outcoupling efficiency of OLEDs.

The improvement of the light outcoupling efficiency of OLEDs has been studied both theoretically [11–21] and experimentally [14, 17]. In order to accurately describe the interaction of emission in OLED with its multilayered and corrugated geometrical structure, numerical simulations are required, for which FDTD models are offering the best scalability and performance on parallel computers. However, large transverse computation domains are necessary so that SPPs propagation and decay is accurately captured. Thus, application of the FDTD for materials with long decay length in optical range is limited, since the computational domain size is restricted by the computer power and memory. Previous FDTD simulations of SPP decay in OLEDs were 2D [14, 16] or included only a fraction of decay length. Since aluminium has shorter decay length it has been simulated in 3D [21].

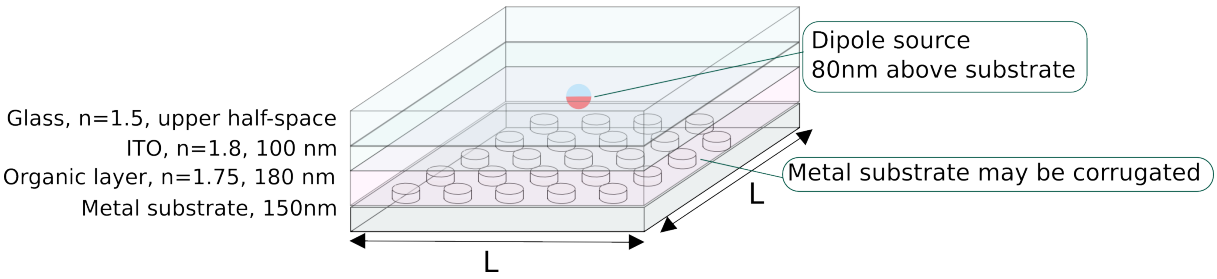

Figure 1. OLED structure in the numerical problem statement

In the current work, we use DTmaxwell code to demonstrate that it is possible to extend the simulation geometry sufficiently so that SPP decay dynamics is accounted for even for materials with long decay length such as silver. We further consider an OLED with periodically corrugated metallic cathode and show how the SPP decay length can be greatly reduced due to scattering off the corrugation. The basic structure of a simulated region is shown in Fig. (Figure 1).

The multi-layered OLED is placed inside a box with the lateral (X and Y) dimensions $L \times L$ (L is a variable numerical parameter). The Z-axis corresponds to the layers normal direction. The bottom layer is a metal substrate, its height is 150 nm. Its dispersion is simulated by the Drude model with the parameters corresponding to silver ($\omega_p = 1.3666 \cdot 10^{16}\text{s}^{-1}$, $\gamma = 2.69 \cdot 10^{13}\text{s}^{-1}$). The second layer is an organic layer with 180 nm height and its refractive index is equal to $n_{org} = 1.75$. The optical wave source is simulated as a point dipole inside this layer, 80 nm above the metal substrate, placed in the center of the computational domain ($x = y = L/2$). Through it a long pulse is injected with central wavelength $\lambda = 550$ nm. Next is ITO layer, its height is equal to 100 nm and $n_{ITO} = 1.8$. Upper halfspace, as well as space around the $L \times L$ box, is treated as glass, $n_g = 1.5$. Corrugation of the cathode is simulated by metal cylinders placed regularly on the cathode surface. This setup corresponds to the one studied in [8], however other types of corrugation (including the random one) may be used.

In order to probe the SPP propagation, the numerical field detectors are placed on the interface between the cathode and the organic layer at regular intervals, along the straight line ($y = L/2$) passing through the c enter of the computational domain ($x = L/2$).

3. Computational considerations

The problem under consideration is essentially multiscale. The mesh step should resolve the smallest scale (cathode skin length is estimated as $\delta_{SPP} \sim 20$ nm under the specified conditions). On the other hand, the transverse size L should be large enough in order to accurately describe the SPP propagation and decay. The SPP decay length is directly related to the SPP dispersion relation at the metal-organic interface $k_{SPP}(\omega)$: $L_{decay} \sim 1/\mathtt{Im}k_{SPP}$, where $k^0_{SPP} = \omega/c\sqrt{(\varepsilon_{org}\varepsilon_m(\omega))/(\varepsilon_{org} + \varepsilon_m(\omega))}$, with ε_m and $\varepsilon_{org} = n^2_{org}$ being the dielectric constants of the metallic and organic layers. For the given material parameters $L_{decay} \sim 50$ mkm.

For the 3D simulation, the necessary numerical parameters are estimated as follows. The mesh step is chosen to be $\Delta x = 5$ nm for the second order scheme in [8]. It is determined by the distance from the dipole to the cathode and the cathode skin length. The time step is limited by the Courant condition and is chosen as $\Delta t \sim 6.7 \cdot 10^{-18}$ s (light velocity is equal to one in the chosen system of units, units for distance are mkm; in this system $\Delta t = 0.002$). The required number of time steps for the light to travel 1 mkm is ~ 500.

Taking all the mentioned limitations into account, the total number of processed Yee cells

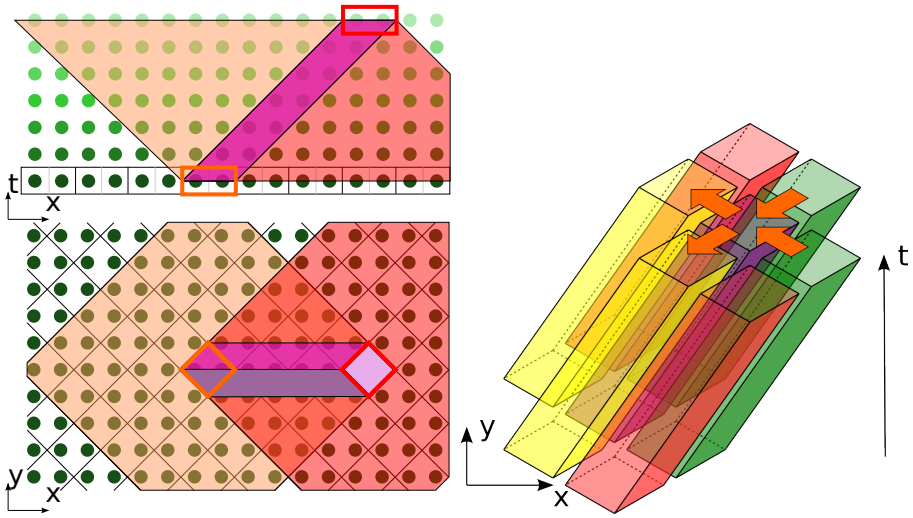

Figure 2. DiamondTorre algorithm. The intersection of domain of influence and domain of dependency of two 2D diamond-shaped bases in 3D time-space (left). Data dependencies between the adjacent DiamondTorres (right). They are directed from green prisms into purple one; from purple prism to yellow prisms. Red and purple prisms calculations are completely independent from each other and may be processed asynchronously.

for the problem (including time steps) should be of the order of 10^{11}. The two following issues stand in the way of efficiently performing such simulations with the traditional FDTD algorithms, especially on GPGPUs. The FDTD simulation is memory-bound. Some popular FDTD codes show sufficient (up to 10^9 Yee cells per second) performance on small sizes, but their performance drops significantly with the increase of data size [22]. This way the accessible problem size is limited by the cumulative GPU device memory, and the CPU RAM (which has much larger size) can not be efficiently utilized. The second issue is that with the use of many-node clusters inter-node data transfers become the limitation of computation time. As a consequence, big domains for SPP problems may not be simulated with the state-of-art solutions, even with the use of the modern supercomputing power.

The algorithm DiamondTorre, which is used in DTmaxwell, provides a solution for the aforementioned issues. The "calculation window" approach allows the use CPU memory and even on-disk swap-file, so the limitation on problem size is lifted by an order of $10 \div 100$. Due to the use of time-space approach, concurrency is implemented in such way that data transfers are completely concealed by computation. These concepts are explained below.

3.1. Time-space approach

DiamondTorre follows the line of LRnLA algorithms: decomposing the discrete time-space computational domains, occupied by Yee cells to be updated, into time-space shapes. These shapes are then processed in the the order satisfying the data dependencies determined by the local stencil used in the discretization of Maxwell's equations. Time-space decomposition allows one to implement processing functions for the shapes that conduct computation on multiple time layers [5, 7]. The prism in Figure 2 represents a decomposition shape for DiamondTorre algorithm — the computation proceeds with the cells, that fall inside it. These cells are on several time layers, but the construction of the algorithm ensures the correct processing order and final computation result.

A row (along the Y axis) of such prisms may be computed asynchronously (red and purple in

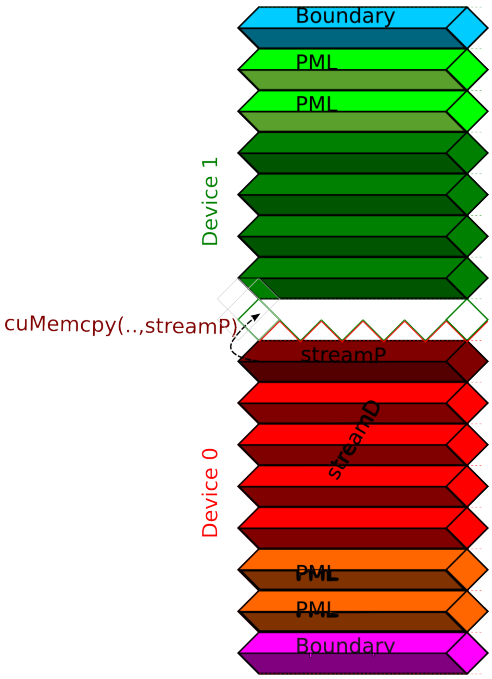

Figure 3. Asynchronous DiamondTorres. The different colors correspond to different CUDA kernels, which are possibly executed on different devices

Figure 2). Several stages of such asynchronous computations propel all cells of the computation mesh forward by a fixed amount of time steps (prism height).

3.2. Calculation window

To perform the DiamondTorre computation only the data that falls into its projection are needed in the device memory. A "calculation window" is implemented, which moves from right to left (according to Figure 2) of the X axis, and encloses an active DiamondTorre at each frame. Data load and save to/from global RAM are performed asynchronously with the computations. Performance does not decline in case the computation time of DiamondTorre is longer than the time, necessary for memory copy to/from the device. Since computation time increases linearly with its height, and the copy time is constant, with the right parameter choice host-device transfers are completely concealed.

3.3. Concurrency on Y axis

Since all DiamondTorre's standing side-by-side along Y axis are asynchronous, they may be processed by different devices inside one node, as well as by different nodes. (fig. 3) In case the number of DiamondTorres per device is high enough, the computation time conceals the data transfer.

As a result, the data transfers may be concealed completely. This alleviates the memory-bound restriction of the numerical scheme. It opens a way for the solution of a new wide range of industrial problems, for which computing power was not enough previously. Algorithm parameters (such as the prism height and problem size) allow not only qualitative but also quantitative estimates of the performance and parallel scaling.

4. Performance evaluation

The performance evaluation in [7] has been carried out for a model problem with no physical significance. Thus, the numerical parameters were chosen to show the largest performance possible.

Here we make the performance test for the target problem, which is characterized by

- wide and flat geometry ($Nx = Ny \gg Nz$);
- inclusion of the Drude model dispersion to the material equations
- on-the-fly diagnostics of the physical parameters

The performance measured is $\sim 0.54 \cdot 10^9$ Yee cell updates per second for one K20x GPGPU. One cell data occupies 68 B of memory, so the computation time for different problem sizes may easily be estimated assuming the complete conceal of device to CPU memory copies.

- $10 \times 10 \mu m^2$ domain — 70 GB, 9 hours;
- $20 \times 20 \mu m^2$ domain — 280 GB, 70 hours;
- $40 \times 40 \mu m^2$ domain — 1100 GB, 580 hours .

With the use of multiple GPUs, 100% efficiency parallel scaling was confirmed in the previous study, so, with the use of several devices, the simulation time is divided by their number.

The performance comparison with EMTL [9] code based on traditional algorithms is shown in Figure 4. The performance is measured for the same problem statement. The difference is in the numerical scheme (4th order spatial finite difference is used in DTmaxwell, 2nd order in EMTL). DTmaxwell has been run on one NVIDIA K20x GPGPU at a single workstation, EMTL has been run on 2 nodes (Xeon E5-2690) of the supercomputer MVS-10p of the Joint Supercomputer Center of Russian Academy of Sciences. Formally these two systems have comparable peak floating point performance of approximately of 100 GFlop/s. It can be seen from the comparison, that the performance of DTmaxwell is more than twice higher than that of EMTL. We also stress here that DTmaxwell has been run on a single workstation, which is only possible due to the memory efficient implementation of LRnLA algorithm.

5. Simulation results

We performed two simulations to demonstrate the importance of modelling of OLED's large geometric sizes and to show the effect of regular corrugation in the cathode. The maximum area size that fits into the CPU memory of one computational node (128 GB) is $18 \times 18 \times 0.64$ mkm. The maximal whole OLED size in our simulations is near to 40×40 mkm: 7680×7680×128 Yee cells with space step Δr=5ñm. We performed all simulations with high-order FDTD numerical scheme with accuracy of 4th order in space and 2nd order in time on hybrid cluster computer K100 (Keldysh Institute of Applied Mathematics, RAS) and Tsubame-2.5 supercomputer using several compute nodes.

In all simulations the source is a vertical dipole (E_z component) placed at the center of OLED. The distance between the dipole and cathode is 80 nm. The dipole generates signal with narrow-band spectra of 500 nm wavelength. Sensors on the cathode detect time-varying E_x component of electromagnetic field at different distances r from the center of simulated region. This field component corresponds to the surface plasmon polariton mode (SPP) of the emmited light. Decay of this mode depends on the properties of the cathode. Except for geometrical divergence of SPP wave with the distance r (proportional to $1/r$), this mode is also exponentially absorbed via interaction with cathode. The length of SPP decay can be very large (about 20-40 micromenters) and corrugation of the cathode significantly decreases this length.

The EM-field visualization for the planar OLED is shown in Figure 5. The propagation of SPP may be easily traced on the metal surface. Figure 6 shows the difference between the

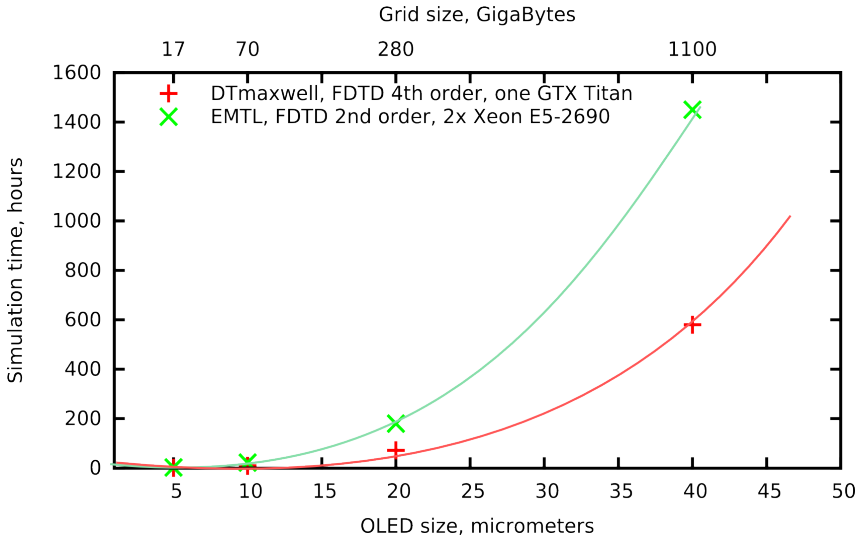

Figure 4. Performance of EMTL (parallel FDTD CPU code based on traditional algorithm) and DTmaxwell (GPGPU code based on LRnLA algorithm) on compute systems of comparable peak performance

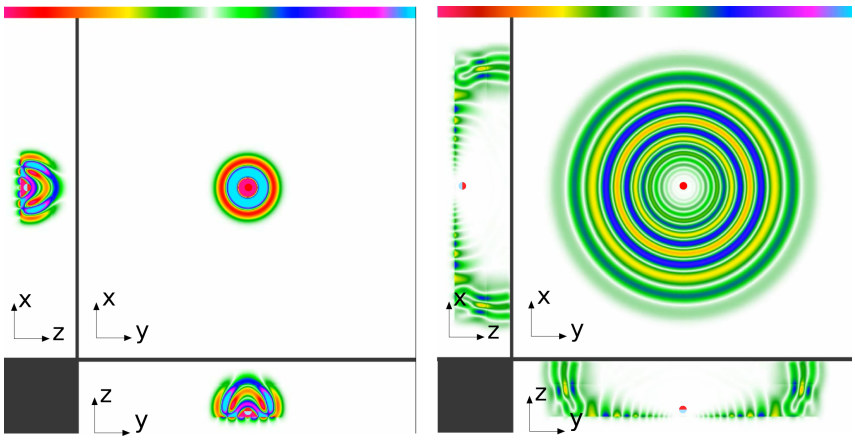

Figure 5. 2D slices of the 3D distribution of the EM field at the two time instants

corrugated and planar OLED. Estimated plasmon decay length is equal to 24 micrometers for the planar structure and only 1.7 micrometers for the corrugated structure.

6. Conclusion

The simulation of OLED geometry for the large area ($40 \times 40 \times 0.64$ mkm) has been performed on clusters of multiple GPGPUs. This way we have confirmed the applicability of DTmaxwell code to large physical problems.

Taking into account the scaling efficiency of the code, we confirm that significantly larger sizes may be simulated with the use of larger GPU clusters. In the simulation, we have traced the SPP propagation and its decay. The result shows that it is necessary to include large domain size in the simulation to reproduce all the relevant SPP phenomena in OLED simulation. The role of the corrugated cathode structure in enhancing the efficiency of light emission from the

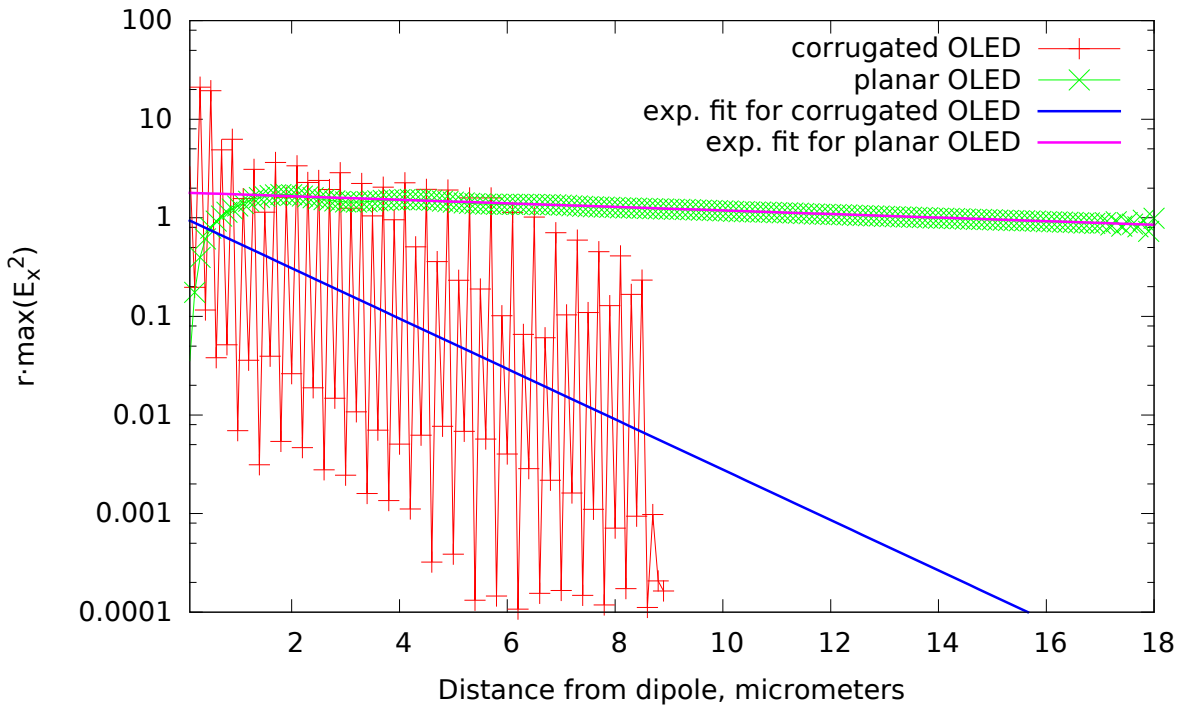

Figure 6. Maximum $|E_x|^2$ component of SPP as a function of the distance from source for planar and corrugated cathodes. The cathode is corrugated with cylindrical holes with depth of 50 nm and diameter of 200 nm. Corrugation period is 400 nm. Fitted lines are proportional to $exp(-r/1.7)$ for the corrugated cathode and $exp(-r/24)$ for the planar OLED (r is measured in micrometers).

OLED, which was studied earlier, is now confirmed by the simulation of much larger scale.

Abbreviations

LRnLA Locally Recursive non-Locally Asynchronous

FDTD Finite Difference Time Domain

PML Perfectly Matched Layer

EM Electro-Magnetic

TF/SF Total Field/Scattered Field

GPGPU General Purpose Graphical Processing Unit

GPU Graphical Processing Unit

SPP Surface Plasmon Polariton

OLED Organic Light Emitting Diode

ITO Indium Tin Oxide

CUDA Compute Unified Device Architecture

References

[1] Ozbay E 2006 *Science* **311** 189–193 ISSN 0036-8075 (*Preprint* `http://science.sciencemag.org/content/311/5758/189.full.pdf`) URL `http://science.sciencemag.org/content/311/5758/189`

[2] Taflove A and Hagness S C 2005 *Computational Electrodynamics: the Finite-Difference Time-Domain Method* 3rd ed (Norwood, MA: Artech House)

[3] Zakirov A 2016 DTmaxwell `https://github.com/zakirovandrey/DTmaxwell4`

[4] Levchenko V 2005 *J. of Inf. Tech. and Comp. Systems* 68

[5] Perepelkina A Y and Levchenko V D 2015 *Keldysh Institute Preprints* **18** 20

[6] Berenger J P 1994 *Journal of Comp. Phys.* **114** 185–200

[7] Zakirov A V, Levchenko V D, Perepelkina A Y and Zempo Y 2016 *Keldysh Institute Preprints* 44–22

[8] Belousov S, Bogdanova M and Teslyuk A 2016 *Journal of Physics D: Applied Physics* **49** 085102

[9] Bogdanova M, Belousov S, Valuev I, Zakirov A, Okun M, Shirabaykin D, Chorkov V, Tokar P, Knizhnik A, Potapkin B, Bagaturyants A, Komarova K, Strikhanov M, Tishchenko A, Nikitenko V, Sukharev V, Sannikova N and Morozov I 2014 *Procedia Computer Science* **29** 740 – 753 ISSN 1877-0509 URL `http://www.sciencedirect.com/science/article/pii/S1877050914002439`

[10] Brütting W, Frischeisen J, Schmidt T D, Scholz B J and Mayr C 2013 *physica status solidi (a)* **210** 44–65 ISSN 1862-6319 URL `http://dx.doi.org/10.1002/pssa.201228320`

[11] Adam J, Hauss J, Gleiss S, Riedel B, Geyer U, Lemmer U and Gerken M 2009 *ICTON Mediterranean Winter Conference, 2009. ICTON-MW 2009. 3rd* (IEEE) pp 1–6

[12] Chutinan A, Ishihara K, Asano T, Fujita M and Noda S 2005 *Organic electronics* **6** 3–9

[13] Kim J W, Jang J H, Oh M C, Shin J W, Cho D H, Moon J H and Lee J I 2014 *Optics express* **22** 498–507

[14] Zhang X L, Feng J, Song J F, Li X B and Sun H B 2011 *Optics letters* **36** 3915–3917

[15] Lee Y J, Kim S H, Kim G H, Lee Y H, Cho S H, Song Y W, Kim Y C and Do Y R 2005 *Optics express* **13** 5864–5870

[16] Kim J Y, Kim D, Kim D H and Choi K C 2014 *IEEE Photonics Technology Letters* **26** 896–899

[17] Nowy S, Krummacher B C, Frischeisen J, Reinke N A and Brütting W 2008 *Journal of Applied Physics* **104** 123109

[18] Qu Y, Slootsky M and Forrest S R 2015 *Nature Photonics* **9** 758–763

[19] Shi X, Wang J, Liu J, Huang S, Wu X, Chen C, Lu J, Su Y, Zheng Y, Kim W Y *et al.* 2014 *Organic Electronics* **15** 864–870

[20] Smith L H, Wasey J A, Samuel I D and Barnes W L 2005 *Advanced Functional Materials* **15** 1839–1844

[21] Sun Y and Forrest S R 2008 *Nature photonics* **2** 483–487

[22] Acceleware Ltd 2016 Acceleware FDTD solvers `http://www.acceleware.com/fdtd-solvers`